Sub-50 fs pulses around 2070 nm from a synchronously-pumped, degenerate OPO

Charles W. Rudy,[1,*] Alireza Marandi,[1] Kirk A. Ingold,[1] Stephen J. Wolf,[1] Konstantin L. Vodopyanov,[1] Robert L. Byer,[1] Lihmei Yang,[2] Peng Wan,[2] and Jian Liu[2]

[1]*Edward L Ginzton Laboratory, Stanford University, 348 Via Pueblo Mall, Stanford, California 94305, USA*
[2]*PolarOnyx, 2526 Qume Drive, San Jose, California 95131, USA*
[*]cwrudy@stanford.edu

Abstract: We report generation of 48 fs pulses at a center wavelength of 2070 nm using a degenerate optical parametric oscillator (OPO) synchronously-pumped with a commercially available 36-MHz, femtosecond, mode-locked, Yb-doped fiber laser. The spectral bandwidth of the output is ~137 nm, corresponding to a theoretical, transform-limited pulse width of 33 fs. The threshold of the OPO is less than 10 mW of average pump power. By tuning the cavity length, the output spectrum covers a spectral width of more than 400 nm, limited only by the bandwidth of the cavity mirrors.

©2012 Optical Society of America

OCIS codes: (190.4975) Parametric processes; (190.4410) Nonlinear optics, parametric processes.

References and links

1. B. E. Carlsten, E. R. Colby, E. H. Esarey, M. Hogan, F. X. Kärtner, W. S. Graves, W. P. Leemans, T. Rao, J. B. Rosenzweig, C. B. Schroeder, D. Sutter, and W. E. White, "New source technologies and their impact on future light sources," Nucl. Instrum. Methods Phys. Res. A **622**(3), 657–668 (2010).
2. N. Leindecker, A. Marandi, R. L. Byer, and K. L. Vodopyanov, "Broadband degenerate OPO for mid-infrared frequency comb generation," Opt. Express **19**(7), 6296–6302 (2011).
3. S. W. Henderson, C. P. Hale, J. R. Magee, M. J. Kavaya, and A. V. Huffaker, "Eye-safe coherent laser radar system at 2.1 µm using Tm,Ho:YAG lasers," Opt. Lett. **16**(10), 773–775 (1991).
4. N. Sugimoto, N. Sims, K. Chan, and D. K. Killinger, "Eye-safe 2.1-Mu m Ho lidar for measuring atmospheric density profiles," Opt. Lett. **15**(6), 302–304 (1990).
5. J. Moses, O. D. Mücke, A. Benedick, E. L. Falcão-Filho, S. W. Huang, K. H. Hong, A. M. Siddiqui, J. R. Birge, F. Ö. Ilday, and F. X. Kärtner, "2-micron optical parametric chirped pulse amplifier for long-wavelength driven high harmonic generation," in *Conference on Lasers and Electro-Optics (CLEO)*, (Optical Society of America, San Jose, CA), paper CTuEE2 (2008).
6. L. E. Myers, R. C. Eckardt, M. M. Fejer, R. L. Byer, W. R. Bosenberg, and J. W. Pierce, "Quasi-phase-matched optical parametric oscillators in bulk periodically poled LiNbO$_3$," J. Opt. Soc. Am. B **12**(11), 2102–2116 (1995).
7. S. T. Wong, T. Plettner, K. L. Vodopyanov, K. Urbanek, M. J. F. Digonnet, and R. L. Byer, "Self-phase-locked degenerate femtosecond optical parametric oscillator," Opt. Lett. **33**(16), 1896–1898 (2008).
8. N. Leindecker, A. Marandi, R. L. Byer, K. L. Vodopyanov, J. Jiang, I. Hartl, M. Fermann, and P. G. Schunemann, "Octave-spanning ultrafast OPO with 2.6-6.1 µm instantaneous bandwidth pumped by femtosecond Tm-fiber laser," Opt. Express **20**(7), 7046–7053 (2012).
9. A. Marandi, N. C. Leindecker, V. Pervak, R. L. Byer, and K. L. Vodopyanov, "Coherence properties of a broadband femtosecond mid-IR optical parametric oscillator operating at degeneracy," Opt. Express **20**(7), 7255–7262 (2012).
10. A. Schmidt, P. Koopmann, G. Huber, P. Fuhrberg, S. Y. Choi, D. I. Yeom, F. Rotermund, V. Petrov, and U. Griebner, "175 fs Tm:Lu$_2$O$_3$ laser at 2.07 µm mode-locked using single-walled carbon nanotubes," Opt. Express **20**(5), 5313–5318 (2012).
11. J. Bethge, J. Jiang, C. Mohr, M. Fermann, and I. Hartl, "Optically referenced Tm-fiber-laser Frequency Comb," in *Lasers, Sources, and Related Photonic Devices Technical Digest*, (Optical Society of America, San Diego, CA, USA, 2012), paper AT5A.3. *http://www.opticsinfobase.org/abstract.cfm?URI=ASSP-2012-AT5A.3*
12. D. A. Bryan, R. Gerson, and H. E. Tomaschke, "Increased optical damage resistance in lithium niobate," Appl. Phys. Lett. **44**(9), 847 (1984).
13. R. L. Byer, "Optical parametric oscillators," in *Quantum Electronics: A Treatise*, H. Rabin and C.L. Tang, eds. (Academic, 1975), 587–702.
14. O. Gayer, Z. Sacks, E. Galun, and A. Arie, "Temperature and wavelength dependent refractive index equations for MgO-doped congruent and stoichiometric LiNbO$_3$," Appl. Phys. B **91**(2), 343–348 (2008).

15. S. Lecomte, R. Paschotta, S. Pawlik, B. Schmidt, K. Furusawa, A. Malinowski, D. J. Richardson, and U. Keller, "Synchronously pumped optical parametric oscillator with a repetition rate of 81.8GHz," IEEE Photon. Technol. Lett. **17**(2), 483–485 (2005).

1. Introduction

There are numerous applications for pulsed 2-µm sources, including laser driven particle acceleration [1], mid- to far-IR spectroscopy [2], "eye-safer" remote sensing [3, 4], high harmonic generation [5], and medical applications, due to the proximity to strong water absorption lines. While development of thulium-doped fiber lasers is still progressing, a clean transfer of the properties of commercial ytterbium-doped fiber lasers to the 2-µm wavelength range can be performed via a degenerate, synchronously- (sync-) pumped OPO with a magnesium oxide-doped, periodically-poled, lithium niobate crystal (MgO:PPLN)—already a mature technology [6]. This concept has been demonstrated at several other pump wavelengths, including 775 nm [7], 1550 nm [2], and 2 µm [8]. Since the output is intrinsically phase- and frequency-locked to the pump source, commercially-available frequency comb sources can be transferred to longer wavelengths [9]. Unlike these previous OPOs, the zero dispersion point of MgO:PPLN at 1.95 µm is near the center wavelength of the OPO, which makes dispersion compensation unnecessary to produce sub-50 fs pulses.

There are various methods of generating ultrashort pulses around the 2-µm wavelength range, including direct (lasers) and nonlinear methods. To the best of our knowledge, current record pulse widths stand at 175 fs from a crystal-based, mode-locked oscillator (Tm:Lu$_2$O$_3$) [10], 65 fs from 2-µm, Tm-doped fiber laser system (mode-locked oscillator and amplifier) [11], and 35 fs from a nonlinear parametric process (optical parametric chirped pulse amplification or OPCPA) centered around 2 µm [5]. While the degenerate OPO method yields shorter pulse widths than either of the mentioned direct methods, the OPCPA nonlinear generation method produces even shorter pulses at the price of complexity. Since the degenerate OPO has a considerably broad parametric gain bandwidth, intracavity dispersion compensation could allow the OPO to surpass the pulse width record while maintaining a relatively straightforward system.

2. Background

A folded bowtie ring cavity was chosen for the design of the sync-pumped, doubly-resonant OPO, shown in Fig. 1. With the repetition rate of the pump—a ~200 fs, PolarOnyx, Yb-doped fiber laser and amplifier system—at ~36.7 MHz, the cavity of the OPO had to be 8.16 m in length to allow for successive roundtrips of the signal to build up. To occupy a reasonable space, the cavity was folded using 10 mirrors—one flat dichroic, dielectric mirror (antireflection or AR coated at the pump wavelength with less than 0.2% reflection and high reflection or HR coated at the signal/idler wavelengths); six flat and two 100 mm radius of curvature (ROC) enhanced gold mirrors; and one ½ inch unprotected gold mirror. The dichroic, dielectric mirror was used for input coupling of the pump. An uncoated, 2-µm thick, nitrocellulose pellicle was used as the output coupler and had an average reflectance of ~4% for the p-polarized signal (and idler; from this point forward, signal refers to both the signal and idler for degenerate operation of the OPO). The total reflectance spectrum of the cavity mirrors is shown in Fig. 2.

The ½ inch gold mirror (in conjunction with the attached piezoelectric transducer or PZT) was used to deliver feedback to the cavity for length stabilization. The separation between the two 100 mm ROC gold mirrors (which create the short arm of the cavity) was close to 101 mm to make the 8.16 m cavity transverse mode stable. Astigmatism due to the Brewster-cut, MgO:PPLN crystal (5 mol%) can cause the transverse mode to be unstable; consequently, a 5 degree angle of incidence on the curved mirrors was used to compensate, creating a cavity length stability range of ~450 µm.
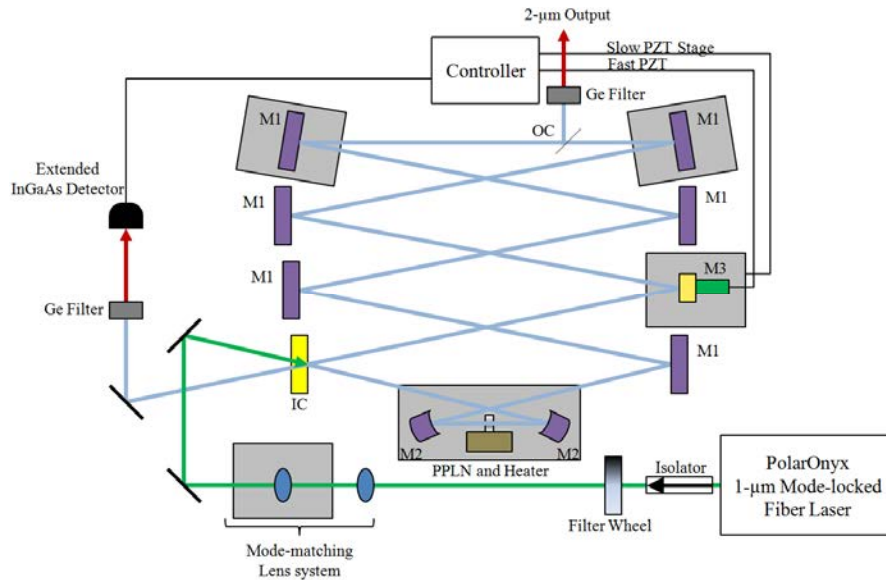
Fig. 1. Schematic of the degenerate OPO. The gray boxed regions depict elements mounted on translation stages. M1: flat enhanced Au mirrors, M2: 100 mm ROC enhanced Au mirrors, M3: ½" Au mirror, IC: Dielectric mirror (HR for signal, AR for pump), OC: 2-µm thick pellicle.

The 1-mm, Brewster-cut, MgO:PPLN crystal was placed in the center of the short arm, where the cavity mode size is the smallest with a ~10 µm beam waist at $1/e^2$ of the peak intensity. The Brewster angle in MgO:PPLN for the signal wavelength was calculated to be 65.46 degrees from normal incidence. The poling period of the MgO:PPLN was calculated to give maximum gain at degeneracy in the case of a 1035 nm pump and crystal temperature of 373 K; the calculated poling period was 31.254 µm. The MgO:PPLN was heated to limit the amount of photorefractive damage caused by the strong 1-µm pump [12]. Figure 2 shows the calculated parametric gain spectrum for three different lengths of the heated, MgO:PPLN crystal in type-0 configuration [13, 14]. As the crystal length is reduced, the gain bandwidth increases at the cost of maximum single pass gain. To reduce the threshold, the 1-mm crystal was used since the gain bandwidth was already larger than the cavity mirror bandwidth.
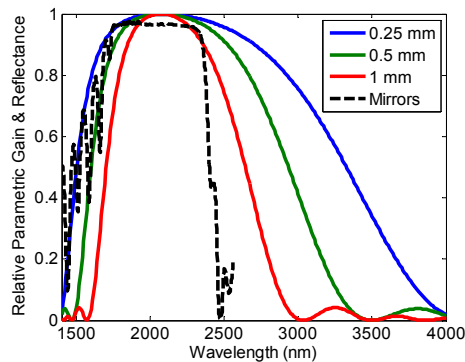

Fig. 2. Normalized parametric gain for varying crystal lengths and reflectance spectrum of the cavity mirrors. The gain bandwidth of 1-mm (red), 0.5-mm (green), and 0.25-mm (blue) MgO:PPLN crystals are shown. The roundtrip cavity mirror reflectance spectrum (without an output coupler) is shown as well (black, dashed).

The mode shape of the 1-µm mode-locked fiber laser output was analyzed and matched to the calculated cavity mode with a two lens system, which consisted of 50 mm and 70 mm AR

coated lenses, to align the cavity shown in Fig. 1. With the mode of the pump set, the cavity mirrors were positioned to allow the pump to propagate through the MgO:PPLN crystal and around the cavity. Leakage through the input coupler was used to monitor spatial overlap between the reflection of the pump from the input coupler and the first roundtrip of the pump. Using a 12-GHz detector and 60-GHz sampling oscilloscope, the temporal overlap of the first roundtrip of the pump and the following reflected pump pulse could be measured to within about one hundred picoseconds for coarse cavity length tuning.

After the initial alignment, the cavity length was swept using a PZT stage with 100 μm of travel at a rate of 5-Hz. The MgO:PPLN crystal was aligned by increasing the visible second harmonic generation (SHG) of the pump. Fine adjustments to the cavity length were achieved with the M1 mirrors mounted on translation stages shown in Fig. 1. The cavity mode and cavity length were tuned until the reflected pump off of the input coupler and leakage of the pump in the cavity through the input coupler interfered. This interference indicated that the cavity was nearly aligned in both length and spatial mode. With the pump interference fringes detected, the cavity length was slightly increased until signs of oscillation were observed—namely pump depletion. The necessary change in cavity length is due to the dispersion introduced by the 1-mm, MgO:PPLN crystal, which causes the cavity to be resonant at slightly different lengths for the pump and the signal (less than 40μm).
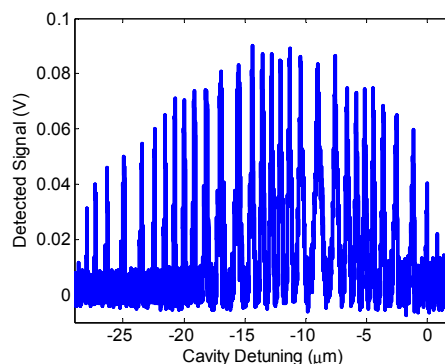

Fig. 3. The oscilloscope trace of the detected OPO signal output versus cavity length, which shows the cavity oscillation peaks. The oscillation peaks corresponding to degenerate operation are on the right side (cavity detuning of ~0 μm), and the OPO operation shifts towards non-degeneracy as the cavity length is reduced. Oscillation peaks from higher order transverse modes can be seen at detected signals below the oscillation peaks from the fundamental mode and contribute to the broadening of the oscillation peaks observed for the cavity detuning around −10 μm.

Due to the doubly-resonant nature of the OPO, it is interferometrically sensitive to the cavity length detuning and oscillates at discrete cavity lengths, leading to "oscillation peaks" shown in Fig. 3 [2]. Once oscillating, a Ge-filtered, extended InGaAs detector was used to monitor the output power in the various oscillation peaks. The spacing between the oscillation peaks, in terms of cavity roundtrip length, is approximately the pump wavelength, around 1 μm [9]. Cavity length stabilization to an oscillation peak was achieved using a "dither" PZT attached to the ½" Au mirror while moving less than 10 nm at ~4 kHz. The cavity length was maintained through a feedback loop with a "dither and lock" servo controller [2]. We were able to operate the OPO stably at several of the oscillation peaks.

3. Results

The minimum threshold of the OPO was extremely low, at less than 10 mW of average pump power; however, as the pump power was increased, the output power did not increase linearly. In fact, at high pump power, the OPO even ceased to oscillate. This is due to the creation of a thermal lens in the crystal at high pump powers. The maximum measured output power of the signal in a single transverse cavity mode (verified using an Ophir thermal

detector) was ~20 mW, which occurred for a nearly degenerate oscillation peak at ~500 mW of incident pump power. The cavity was adjusted in order to operate at this level of pump power, which significantly raised the threshold. Pump depletion was just over 30%; however, pump depletion should approach over 80% [2]. The OPO conversion efficiency can be increased through improving the overlap between the pump and signal spatial modes by taking into account the created thermal lens.
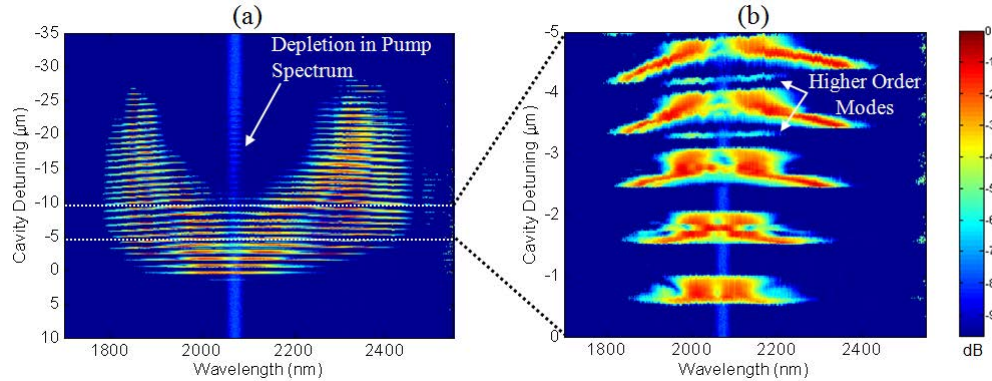

Fig. 4. The normalized spectra of the OPO output versus cavity detuning length are shown in (a) and (b). (a) The degenerate oscillation peaks are at the bottom (cavity detuning of ~0 µm), while the non-degenerate peaks are at the top (cavity detuning of ~-20 µm). (b) The spectra for cavity detuning lengths near degeneracy (cavity detuning of 0 to 5 µm) from (a) are shown in greater detail, allowing for observation of the oscillation peaks from higher order transverse modes. The second order of the pump spectrum can be seen as a vertical line in (a) and (b) around 2070 nm. Depletion of the pump is visible in (a). Note: The peaks in the spectra are ~10 dB above the noise floor.

Figure 4 shows the OPO spectrum for varying cavity length as measured with an $f = 20$ cm monochromator. The oscillation peaks cover several modes of operation of the OPO, including both degenerate and non-degenerate oscillation. In Fig. 4(a), the degenerate oscillation peaks, where the signal and idler are indistinguishable, are towards the bottom of the figure or at longer cavity lengths, while the non-degenerate oscillation peaks, where the signal and idler are completely separated, are at the top of the figure or at shorter cavity lengths. The oscillation peaks in the region in between degenerate and non-degenerate operation are referred to as nearly degenerate. The power in the oscillation peaks is highest around these nearly degenerate peaks, which are spectrally broad. The power then declines as the oscillation peaks approaches degeneracy or completely non-degenerate oscillation (where the signal and idler approach the edges of the mirror bandwidth), which can be observed in the varying detected power of the oscillation peaks in the oscilloscope trace in Fig. 3. The constant signal in the center of the spectrum (vertical line at ~2070 nm in Fig. 4) is the second order deflection of the pump spectrum at the grating. Pump depletion can most easily be seen in this signal in Fig. 4(a) at the cavity lengths where the OPO oscillates non-degenerately (where the signal/idler spectrum and second order pump spectrum do not overlap). When closely examining one of the oscillation peaks in Fig. 4(b), the signal spectrum noticeably changes with cavity detuning within an oscillation peak. This implies that the spectra of the peaks are greatly influenced by dispersion in the cavity.

Upon further inspection of the spectra near degeneracy in Fig. 4(b), smaller peaks in between the main oscillation peaks are noticeable. These peaks are caused by higher order transverse modes that oscillate in the cavity. In previous sync-pumped, degenerate OPOs [2, 7, 8], these peaks were not observed due to limited pump power (and less distortion of the spatial mode of the pump due to thermal lensing); however, tuning the cavity configuration can cause these peaks to become even stronger than the fundamental transverse mode's oscillation peaks. Gain for the higher order modes may be partially caused by the presence of

higher order spatial modes in the pump. These higher order spatial mode oscillation peaks are also observable in the oscilloscope trace in Fig. 3 as broadening of the oscillation peaks.
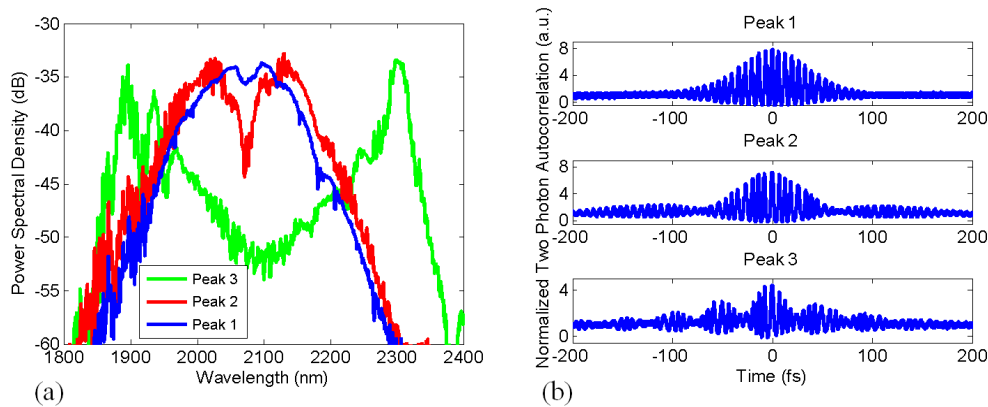

Fig. 5. (a) Spectrum and (b) autocorrelation for individual oscillation peaks. (a) The spectrum for the degenerate peak (peak 1, blue) shows only a slight dip in the center of the spectrum (<2 dB), while the "nearly" non-degenerate peaks (such as peak 3, green) have a clear splitting between signal and idler. This splitting results in the modulation of the autocorrelation trace. (b) The autocorrelation traces were measured after a 200-μm thick Ge-filter. Peak 1 corresponds to the longest cavity length shown in Fig. 4(b), peak 2 is ~2 μm shorter in cavity length, while peak 3 is one of the oscillation peaks in the transition region between degenerate and non-degenerate oscillation. Note: The autocorrelation trace of peak 3 has a reduced peak to background ratio.

Tuning from degeneracy to non-degenerate oscillation clearly affects both the spectrum and autocorrelation. Figure 5(a) depicts the spectra of selected peaks as measured with a Yokogawa AQ6375 optical spectrum analyzer. One can see that at degeneracy, the spectrum is a single peak (peak 1), and the spectrum splits after tuning the DC offset of the feedback loop to the nearly degenerate region (peak 3). As previously mentioned, this split in spectrum can be seen as a separation of the signal and idler, which results in modulation of the OPO pulse in the time domain. For example, the overlap in the spectrum around the point of degeneracy for peak 3 in Fig. 5(a) allows for the signal and idler to remain coherent, which introduces temporal distortion of the output pulse clearly seen in the autocorrelation trace in Fig. 5(b). At degeneracy (peak 1), the measured pulse width from the autocorrelation shown in Fig. 5(b) is 48 fs, assuming a sech^2 pulse intensity profile, with ~137 nm of spectral bandwidth, which makes the time-bandwidth-product 0.46.
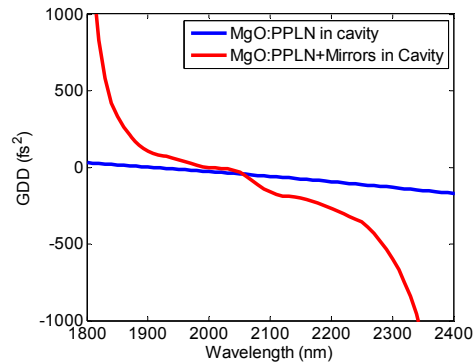

Fig. 6. Roundtrip GDD for two cases: (blue curve) the GDD for 1 mm of MgO:PPLN and (red curve) the GDD of the same crystal including the GDD of the coated mirrors. The degeneracy point is at ~2070 nm.

Shorter pulses could be achieved if compensation for dispersion introduced by the mirrors is explored; theoretically, pulses ~33 fs for the measured bandwidth could be generated. There was no dispersion compensation within the cavity, making the signal spectral bandwidth limited by dispersion. Figure 6 shows the group delay dispersion (GDD, $\partial^2\varphi/\partial\omega^2$) of one roundtrip in the cavity for the crystal and mirrors. The material zero-dispersion point of MgO:PPLN is at 1.95 μm (hence GDD is dominated by the dielectric mirrors), which makes dispersion compensation unnecessary for achieving sub 50-fs pulses.

When the cavity was shifted towards non-degeneracy, the spectral bandwidth expands to ~430 nm (outer 3dB bandwidth of peak 3 with a −15 dB dip in the center of the spectrum). This was about the bandwidth of the coated mirrors in the cavity. The width of the main lobe of the autocorrelation trace was measured to be 21 fs, achieving a time-bandwidth product of 0.632. This broad signal bandwidth demonstrates the extent of the gain bandwidth of the OPO. If flattening of the roundtrip GDD (Fig. 6) with proper dispersion compensation could be achieved, this gain bandwidth could be used to generate a pulse width of only a few optical cycles at degeneracy.

4. Conclusions and future work

A degenerate sync-pumped OPO was able to generate less than 50-fs wide pulses at ~10 mW of average output power. For nearly degenerate oscillation, the signal output spectrum had a bandwidth of 430 nm, with ~20 mW of average output power. Shortening the cavity by using a source with a higher repetition rate [15] should help improve stability. Degenerate operation of the OPO provides pulses of shorter duration than direct methods of producing 2-μm pulses, making it a viable alternative as a broadband source in this wavelength range for numerous applications. With the large gain bandwidth demonstrated, dispersion compensation of the cavity could make a few-cycle pulse potentially possible.

Acknowledgments